Journal of the American College of Cardiology Vol. 58, No. 19, 2011

Published by Elsevier Inc.
ISSN 0735-1097/$36.00
doi:10.1016/j.jacc.2011.06.066

Cardiac Imaging

Diagnosis of Ischemia-Causing Coronary Stenoses by Noninvasive Fractional Flow Reserve Computed From Coronary Computed Tomographic Angiograms

Results From the Prospective Multicenter DISCOVER-FLOW (Diagnosis of Ischemia-Causing Stenoses Obtained Via Noninvasive Fractional Flow Reserve) Study

Bon-Kwon Koo, MD, PhD,* Andrejs Erglis, MD, PhD,† Joon-Hyung Doh, MD, PhD,‡ David V. Daniels, MD,§ Sanda Jegere, MD,‖ Hyo-Soo Kim, MD, PhD,* Allison Dunning, MD,¶ Tony DeFrance, MD,# Alexandra Lansky, MD,** Jonathan Leipsic, BSc, MD,†† James K. Min, MD‡‡

Seoul and Goyang, South Korea; Riga, Latvia; Palo Alto, San Francisco, and Los Angeles, California; New York, New York; New Haven, Connecticut; and Vancouver, British Columbia, Canada

Objectives The aim of this study was to determine the diagnostic performance of a new method for quantifying fractional flow reserve (FFR) with computational fluid dynamics (CFD) applied to coronary computed tomography angiography (CCTA) data in patients with suspected or known coronary artery disease (CAD).

Background Measurement of FFR during invasive coronary angiography is the gold standard for identifying coronary artery lesions that cause ischemia and improves clinical decision-making for revascularization. Computation of FFR from CCTA data (FFR_{CT}) provides a noninvasive method for identifying ischemia-causing stenosis; however, the diagnostic performance of this new method is unknown.

Methods Computation of FFR from CCTA data was performed on 159 vessels in 103 patients undergoing CCTA, invasive coronary angiography, and FFR. Independent core laboratories determined FFR_{CT} and CAD stenosis severity by CCTA. Ischemia was defined by an FFR_{CT} and FFR $\leq$0.80, and anatomically obstructive CAD was defined as a CCTA with stenosis $\geq$50%. Diagnostic performance of FFR_{CT} and CCTA stenosis was assessed with invasive FFR as the reference standard.

Results Fifty-six percent of patients had $\geq$1 vessel with FFR $\leq$0.80. On a per-vessel basis, the accuracy, sensitivity, specificity, positive predictive value, and negative predictive value were 84.3%, 87.9%, 82.2%, 73.9%, 92.2%, respectively, for FFR_{CT} and were 58.5%, 91.4%, 39.6%, 46.5%, 88.9%, respectively, for CCTA stenosis. The area under the receiver-operator characteristics curve was 0.90 for FFR_{CT} and 0.75 for CCTA ($p = 0.001$). The FFR_{CT} and FFR were well correlated ($r = 0.717$, $p < 0.001$) with a slight underestimation by FFR_{CT} (0.022 ± 0.116, $p = 0.016$).

Conclusions Noninvasive FFR derived from CCTA is a novel method with high diagnostic performance for the detection and exclusion of coronary lesions that cause ischemia. (The Diagnosis of ISChemia-Causing Stenoses Obtained Via NoninvasivE FRactional FLOW Reserve; NCT01189331) (J Am Coll Cardiol 2011;58:1989–97) © 2011 by the American College of Cardiology Foundation

From the *Department of Medicine, Seoul National University Hospital, Seoul, South Korea; †Department of Medicine, Pauls Stradins Clinical University Hospital, Riga, Latvia; ‡Department of Medicine, Inje University Ilsan Paik Hospital, Goyang, South Korea; §Department of Medicine, Stanford University School of Medicine, Palo Alto, California; ‖Division of Cardiology, Pauls Stradins Clinical University Hospital, Riga, Latvia; ¶Department of Public Health, Weill Cornell Medical College, New York, New York; #CVCTA, San Francisco, California; **Yale University School of Medicine, New Haven, Connecticut; ††Department of Radiology, St. Paul's Hospital, Vancouver, British Columbia, Canada; and the ‡‡Cedars-Sinai Heart Institute, Cedars-Sinai Medical Center, Los Angeles, California. Dr. DeFrance is on the Speaker's Bureau of Toshiba Medical Systems. Dr. Leipsic is on the Speaker's Bureau and medical advisory board of GE Healthcare. All other authors have reported that they have no relationships relevant to the contents of this paper to disclose.

Manuscript received April 20, 2011; revised manuscript received June 21, 2011, accepted June 27, 2011.

JACC Vol. 58, No. 19, 2011
November 1, 2011:1989–97

Abbreviations and Acronyms

AUC = area under the receiver-operator characteristics curve

CABG = coronary artery bypass surgery

CAD = coronary artery disease

CCTA = coronary computed tomographic angiography

CFD = computational fluid dynamics

FFR = fractional flow reserve

FFR_{CT} = computation of fractional flow reserve from coronary computed tomographic angiography data

ICA = invasive coronary angiography

Large-scale randomized trials have demonstrated that fractional flow reserve (FFR)—or the ratio of maximal myocardial blood flow through a diseased artery to the blood flow in the hypothetical case that this artery is normal—is a useful physiological test for assessment of lesion-specific ischemia and a valuable adjunct to anatomic assessment of coronary artery disease (CAD) as determined by invasive coronary angiography (ICA) (1–4). This combined anatomic-physiological evaluation of CAD allows for enhanced clinical decision-making that improves event-free survival, reduces unnecessary revascularization, and lowers healthcare costs (5,6).

Coronary computed tomographic angiography (CCTA) has emerged as a noninvasive test that assesses anatomic CAD stenosis severity (7). Although prior multicenter studies have demonstrated favorable diagnostic performance for CCTA identification and exclusion of anatomically obstructive coronary stenoses, CAD stenosis by CCTA demonstrates an unreliable relationship to lesion-specific ischemia, with the majority of high-grade stenoses detected by CCTA not causal of ischemia (8–11). These findings have raised concerns that widespread use of CCTA might result in excess referral of patients to ICA and unnecessary revascularization of nonischemic coronary lesions (12,13).

See page 1998

Computational fluid dynamics (CFD), as applied to CCTA images, represents a novel method that enables prediction of blood flow and pressure fields in coronary arteries and calculation of lesion-specific FFR (14–16). The FFR can be computed from typically acquired CCTA scans (FFR_{CT}) without any modification of CCTA protocols, additional image acquisition, or administration of medications.

We performed a prospective multicenter study to compare the diagnostic performance of FFR_{CT} with CCTA stenosis for the diagnosis of lesion-specific ischemia, as determined by FFR performed at the time of ICA.

Methods

Study design. The DISCOVER-FLOW (Diagnosis of ISChemia-Causing Stenoses Obtained Via NoninvasivE FRactional FLOW Reserve) study was conducted at 4 sites (Seoul National University Hospital, Seoul, Korea; Pauls Stradins Clinical University Hospital, Riga, Latvia; Inje University Ilsan Paik Hospital, Goyang, Korea; Stanford University Medical Center, Palo Alto, California). The study protocol was approved by the Institutional Review Boards of each center. The study was funded by Heartflow, Inc. (Redwood City, California).

Study population. The study population comprised 103 stable patients with suspected or known CAD who underwent CCTA, ICA, and FFR between October 13, 2009, and January 14, 2011. Inclusion criteria were: adult ≥18 years of age, CCTA with ≥50% stenosis in a major coronary artery ≥2.0 mm diameter (determined by clinical site), and undergoing clinically indicated ICA with FFR. Exclusion criteria included individuals unable to provide informed consent; noncardiac illness with life expectancy <2 years; pregnant state; allergy to iodinated contrast; serum creatinine ≥1.7 mg/dl; significant arrhythmia; heart rate ≥100 beats/min; systolic blood pressure ≤90 mm Hg; contraindication to beta blockers, nitroglycerin or adenosine; prior coronary artery bypass surgery (CABG); Canadian Cardiovascular Society class IV angina; or non-evaluable CCTA as determined by the CCTA core laboratory. Importantly, every evaluable CCTA as judged by the CCTA core laboratory was interpreted in independent blinded fashion by the FFR_{CT} core laboratory in an intent-to-diagnose fashion.

Protocol for CCTA. Each center performed CCTA in accordance with the Society of Cardiovascular Computed Tomography Guidelines on Performance of CCTA with a variety of different computed tomography scanner platforms (Lightspeed VCT, GE Healthcare, Milwaukee, Wisconsin; Somatom Sensation and Definition CT, Siemens, Forchheim, Germany; Brilliance 256 and 64, Philips, Surrey, United Kingdom; Aquilion One and 64, Toshiba, Otawara, Japan) (17). Intravenous or oral metoprolol was administered for any patient with a heart rate ≥65 beats/min. Immediately before image acquisition, 0.2 mg sublingual nitroglycerin was administered. During acquisition, 80 to 100 cc of contrast (Isovue 370 mg/dl, Bracco, Princeton, New Jersey; Omnipaque 350 mg/dl, GE Healthcare, Princeton, New Jersey; Visipaque 320 mg/dl, GE Healthcare) was injected, followed by a saline flush. Helical or axial scan data were obtained with retrospective or prospective electrocardiographic gating, respectively. Image acquisition was prescribed to include the coronary arteries, left ventricle, and proximal ascending aorta. The scan parameters were: 64 × 0.625/0.750 mm collimation, tube voltage 100 or 120 mV, effective 400 to 650 mA. Radiation dose reduction strategies were employed when feasible, and doses ranged from 3 to 15 mSv.

Noninvasive coronary artery analysis by CCTA. The CCTAs were analyzed in blinded fashion by an independent core laboratory (CVCTA, San Francisco, California) in accordance with the Society of Cardiovascular Computed Tomography guidelines on CCTA interpretation (18). The CCTA images were evaluated with 3-dimensional workstations (Vital Images, Minneapolis, Minnesota; Ziosoft, Redwood City, California). The CCTAs were visualized by any post-

processing method, including axial, multiplanar reformat, maximum intensity projection, and cross-sectional analysis.

Coronary segments were scored in a semi-quantitative manner with an 18-segment Society of Cardiovascular Computed Tomography model. In each segment, atherosclerosis was defined as tissue structures >1 mm^2 that existed within the coronary artery lumen or adjacent to the coronary lumen that could be discriminated from pericardial tissue, epicardial fat, or vessel lumen itself. Coronary lesions were quantified for luminal diameter stenosis as none (0%), mild (1% to 49%), moderate (50% to 69%), or severe (≥70%). Anatomically obstructive CAD by CCTA was defined at 2 thresholds (≥50% or ≥70% stenosis severity) on a per-patient and per-vessel basis.

ICA image acquisition and FFR performance. Selective ICA was performed by standard catheterization in accordance with the American College of Cardiology Guidelines for Coronary Angiography (19). Two projections were obtained/major epicardial vessel, with angles of projection optimized on the basis of cardiac position. The FFR was performed in vessels as clinically indicated but was not performed for subtotal (99% stenosis) lesions. After administration of nitroglycerin, a pressure-monitoring guidewire (PressureWire Certus, St. Jude Medical Systems, Uppsala, Sweden; ComboWire, Volcano Corporation, San Diego, California) was advanced past the stenosis. Hyperemia was attained by administration of intravenous (140 μg/kg/min, n = 90) or intracoronary (50 μg, n = 13) adenosine, with route of administration at the discretion of the operator (20). The position of the distal pressure sensor was recorded to enable the FFR_{CT} to be calculated from the same point as the measured FFR. The FFR was calculated by dividing the mean distal coronary pressure by the mean aortic pressure during hyperemia. The FFR was considered diagnostic of ischemia at a threshold of ≤0.80 on a per-patient and per-vessel basis (3).

FFR_{CT} interpretation. The FFR_{CT} was performed in blinded fashion by core laboratory scientists at HeartFlow, Inc. (Redwood City, California). Three-dimensional models of the coronary tree and ventricular myocardium were reconstructed with custom methods applied to blinded CCTA data for simulation of coronary flow and pressure (14). Blood was modeled as a Newtonian fluid with incompressible Navier-Stokes equations and solved subject to appropriate initial and boundary conditions with a finite element method on a parallel supercomputer. Because coronary flow and pressure are unknown a priori, a method to couple lumped parameter models of the microcirculation to the outflow boundaries of the 3-D model was used (21). The FFR_{CT} analyses required approximately 5 h/exam; iterative improvements in automation are expected to reduce processing time.

The FFR_{CT} technology is based on 3 key principles. Because patients with rest angina were excluded, the first is that coronary supply meets myocardial demand at rest. Adherence to this principle enabled calculation of total resting coronary flow relative to ventricular mass. The second principle is that resistance of the microcirculation at rest is inversely but not linearly proportional to the size of the feeding vessel (22–26). The third principle is that microcirculation reacts predictably to maximal hyperemic conditions in patients with normal coronary flow (27). On the basis of these principles, a lumped parameter model representing the resistance to flow during simulated hyperemia was applied to each coronary branch of the segmented CCTA model. The FFR_{CT} was modeled for conditions of adenosine-induced hyperemia; an FFR_{CT} ≤0.80 was considered diagnostic of lesion-specific ischemia.

The FFR_{CT} core laboratory scientists were instructed as to the location within a coronary artery where the FFR was reported by an independent scientist who interpreted both the CCTA and ICA and who was not involved in the CCTA, ICA, FFR_{CT}, or FFR analyses. The FFR_{CT} core laboratory scientists interpreted all CCTAs judged evaluable by an independent blinded reader in an intent-to-diagnose fashion.

Sample size calculation and statistical analyses. The diagnostic accuracy of CCTA stenosis ≥50% for the detection of lesion-specific ischemia as compared with FFR was estimated to be 49% (11). To detect a relative improvement in diagnostic accuracy of ≥25% for FFR_{CT} as compared with CCTA stenosis, 150 vessels provided 90% power with a 2-sided alternative hypothesis. For estimation of power, we employed McNemar's test to account for the paired nature of the data and assumed independence of lesion-specific ischemia in vessels and a 22% rate of discordance between FFR_{CT} and FFR.

Categorical variables are presented as frequencies and percentages, with continuous variables as mean ± SD. Diagnostic measures on a per-patient and -vessel basis were calculated, including sensitivity, specificity, positive predictive value (PPV), negative predictive value (NPV), accuracy, positive likelihood ratio, and negative likelihood ratio. The area under the receiver-operator characteristics curve (AUC) was calculated for CCTA stenosis and FFR_{CT}. The AUCs were compared by the DeLong method. Pearson's and Spearman's correlation coefficients were calculated to determine the relationship between FFR_{CT} and FFR. Bland-Altman analysis was performed with FFR as the standard of reference. All analyses were performed with SAS Proprietary Software (version 9.2, SAS Institute, Cary, North Carolina).

Results

Patient characteristics. One hundred three patients (100%) who underwent ICA, FFR, CCTA, and blinded CCTA core laboratory evaluation comprised the study population. Baseline characteristics are listed in Table 1. The mean interval between the CCTA and FFR was 2.3 days (range 0 to 26 days), with no adverse events or revascularization between exams. Six vessels were subtotally occluded (99% stenosis), and FFR was not measured

JACC Vol. 58, No. 19, 2011
November 1, 2011:1989–97

Table 1 Baseline Characteristics

Mean age, yrs	62.7 (8.5)
Male	74 (72)
Caucasian (%)	34 (33)
Hypertension	67 (65)
Hyperlipidemia	67 (65)
Diabetes	26 (26)
Mean body-mass index	25.8 (3.5)
Current smoker	24 (36)
Cardiovascular history	
Prior myocardial infarction	17 (17)
Prior PCI	16 (16)
Prior CABG	0 (0)
Left ventricular ejection fraction, %	62.3 (5.7)
Vital signs*	
Systolic blood pressure, mm Hg	139.1 (17.6)
Diastolic blood pressure, mm Hg	80.9 (11.4)
Heart rate, beats/min	63.9 (8.5)
Laboratory measures	
Hemoglobin, mg/dl	14 (1.6)
Hematocrit, %	41.2 (4.3)
Creatinine, mg/dl	0.97 (0.18)
Medications	
Aspirin	43 (87.8)
Beta-blocker	54 (96.4)
Nitrate	41 (64.1)
Statins	44 (89.8)
ACE inhibitors	39 (86.7)
Calcium-channel blockers	38 (86.7)
Clopidogrel	79 (94.1)
ARBs	5 (10.2)
Other medication	18 (36.7)

Values are n (%). *At time of coronary computed tomographic angiography.

ACE = angiotensin-converting enzyme; ARB = angiotensin receptor blocker; CABG = coronary artery bypass surgery; PCI = percutaneous coronary intervention.

in these vessels. Of the 159 vessels for which FFR was performed, maximal stenoses as determined by the CCTA core lab were: 0% (n = 7); 1% to 25% (n = 20); 26% to 50% (n = 18); 50% to 69% (n = 47); and 70% to 98% (n = 67).

Diagnostic performance of FFR_{CT} versus CCTA for diagnosis of ischemia-producing lesions. The FFR_{CT} applied to coronary vessels resulted in 51 true positives (32.1%), 83 true negatives (52.2%), 18 false positives (11.3%), and 7 false negatives (4.4%). Diagnostic performance of FFR_{CT} and CCTA on a patient- and vessel-based evaluation are listed in Table 2. Representative examples of anatomically obstructive stenosis with and without ischemia-producing stenoses are shown in Figures 1 and 2. Applying FFR_{CT} values and CCTA stenosis ranges revealed a higher AUC for FFR_{CT} as compared with CCTA (0.90 vs. 0.75, p = 0.001) on a lesion-specific basis (Fig. 3). Per-patient performance of FFR_{CT} versus CCTA can be seen in Table 2. A higher AUC for FFR_{CT} was observed, similar to per-vessel analyses, as compared with CCTA for per-patient discrimination (0.92 vs. 0.70, p = 0.0001) (Fig. 3). No improvement in AUC was observed on either the per-vessel and per-patient level when CCTA stenosis was added to FFR_{CT} (p = 0.50 and p = 0.64, respectively).

Per-vessel diagnostic performance of FFR_{CT} in vessels with intermediate stenoses by CCTA. Among the 47 vessels with 50% to 69% stenoses by CCTA, 25.5% (n = 12) exhibited ischemia FFR. For these stenoses, FFR_{CT} demonstrated a diagnostic accuracy, sensitivity, specificity, PPV, and NPV of 83.0%, 66.7%, 88.6%, 66.7%, and 88.6%. All 4 "false negative" vessels, where FFR_{CT} did not demonstrate ischemia, had measured FFR values between 0.75 and 0.80.

Correlation of FFR_{CT} to FFR. There was good correlation of per-vessel FFR_{CT} values with FFR values (Spearman's rank correlation = 0.717, p < 0.0001; Pearson's correlation coefficient = 0.678, p < 0.0001), with a slight underestimation of FFR_{CT} as compared with measured FFR (mean difference 0.022 ± 0.116, p = 0.016) (Figs. 4 and 5) at the per-vessel level, with similar values and no systematic differences at the per-patient level (mean difference 0.019 ± 0.128, p = 0.131).

Discussion

In this prospective multicenter study comparing FFR_{CT} with CCTA stenosis in patients undergoing ICA and FFR, the diagnostic accuracy of FFR_{CT} was superior and additive to CCTA stenosis for the diagnosis of ischemia-causing lesions as determined by an invasive FFR reference standard. The FFR_{CT} augmented the discriminatory ability to

Table 2 Diagnostic Performance of FFR_{CT} and CCTA on a Per-Vessel and -Patient Basis

	Per-Vessel		Per-Patient	
Measure	FFR_{CT} ≤0.80 (95% CI)	CCTA Stenosis ≥50% (95% CI)	FFR_{CT} ≤0.80 (95% CI)	CCTA Stenosis ≥50% (95% CI)
Accuracy	84.3 (77.7–90.0)	58.5 (50.4–66.2)	87.4 (79.4–93.1)	61.2 (51.1–70.6)
Sensitivity	87.9 (76.7–95.0)	91.4 (81.0–97.1)	92.6 (82.1–97.9)	94.4 (84.6–98.8)
Specificity	82.2 (73.3–89.1)	39.6 (30.0–49.8)	81.6 (68.0–91.2)	24.5 (13.3–38.9)
PPV	73.9 (61.9–83.7)	46.5 (37.1–56.1)	84.7 (73.0–92.8)	58.0 (47.0–68.4)
NPV	92.2 (84.6–96.8)	88.9 (75.9–96.3)	90.9 (78.3–97.5)	80.0 (51.9–95.7)
LR (+)	4.94 (3.54–6.89)	1.51 (1.33–1.73)	5.03 (3.34–7.59)	1.25 (1.11–1.41)
LR (−)	0.147 (0.097–0.224)	0.22 (0.127–0.370)	0.091 (0.046–0.181)	0.229 (0.097–0.541)

For this analysis, a fractional flow reserve or computation of fractional flow reserve from coronary computed tomographic angiography data (FFR_{CT}) ≤0.80 was diagnostic of lesion-specific ischemia, and a coronary computed tomographic angiography (CCTA) stenosis ≥50% was anatomically obstructive.

CI = confidence interval; LR(+) = positive likelihood ratio; LR(−) = negative likelihood ratio; NPV = negative predictive value; PPV = positive predictive value.

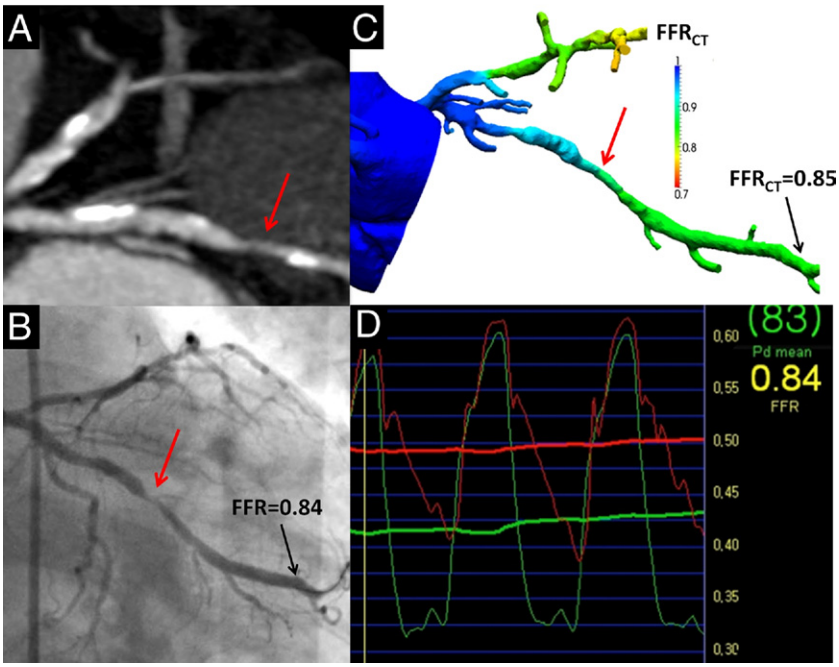

Figure 1 **Anatomically Obstructive Stenosis With No Functional Ischemia**

(A) Coronary computed tomography angiography demonstrating obstructive (≥50%) stenosis **(white arrow)** in the obtuse marginal (OM) branch of the left circumflex artery. Proximal and distal to the lesion, there are multiple areas of diffuse calcified plaque of intermediate stenosis severity (40% to 69%). **(B)** Invasive coronary angiography confirms the obstructive OM stenosis **(red arrow)**. **(C)** Computation of fractional flow reserve from coronary computed tomographic angiography data (FFR$_{CT}$) demonstrates no ischemia in the OM, with a computed value of 0.85. **(D)** Fractional flow reserve (FFR) of 0.84 at the time of invasive coronary angiography similarly demonstrates no ischemia in the OM.

identify lesions that cause ischemia, as compared with CCTA stenosis, largely by reducing the rates of false positive lesions incorrectly classified by stenosis alone.

To our knowledge, this study represents the first of its kind to evaluate CFD principles applied to CCTA images for derivation of patient-specific measures of coronary artery pressure. Importantly, the calculation of FFR$_{CT}$ required no modification of CCTA acquisition protocols, no additional imaging, and no additional administration of medications. The results of the present study establish the feasibility of CFD modeling for noninvasive determination of the physiological consequences of CAD and support a utility for application of FFR$_{CT}$ in patients undergoing CCTA.

Coronary computed tomographic angiography is a noninvasive test for anatomic assessment of CAD severity that has been suggested as an alternative to ICA (8–10,28). Prior CCTA studies employing computed tomography scanners with ≥64-detector rows have observed a generally high diagnostic performance of CCTA, as compared with quantitative coronary angiography as a reference standard. However, significant false positive rates underscore a general overestimation of CAD severity by CCTA, and even among obstructive CAD lesions identified by CCTA that are confirmed at ICA, only a minority of such lesions are causal of ischemia (8,10,11). These findings have also been observed for ICA, and prior multicenter studies support a distinct benefit for adjunctive physiological assessment of anatomic CAD stenoses by FFR (3,5,6,29). In the FAME (Fractional Flow Reserve versus Angiography for Multivessel Evaluation) study of 1,005 patients with multivessel CAD, those that underwent FFR-guided revascularization—as compared with patients undergoing anatomically guided revascularization—experienced lower rates of adverse events, placement of fewer coronary stents, and lower healthcare costs (3,5). In this regard, the addition of FFR$_{CT}$ to CCTA might improve clinical decision-making and promote salutatory outcomes for individuals with CCTA-identified CAD; prospective outcomes studies are warranted.

We employed definitions identical to those used in the FAME study for ischemia by FFR (≤0.80) and obstructive stenosis by angiography (≥50%) (3). Prior studies have demonstrated enhanced specificity for detection of ischemia when employing an FFR threshold of ≤0.75 or a stenosis threshold of ≥70%, albeit at a penalty of increased false negatives (30). We examined the relationship of an FFR$_{CT}$ cutoff of 0.75 and CAD stenosis of 50%, respectively, and found similar results (data not shown).

One distinction between our study and the FAME study is how we dealt with subtotal (99%) occlusions. In the FAME study, these lesions were not subjected to FFR for reasons of safety and were assigned a value of 0.50 (3). We identified 6 vessels with subtotal occlusions in our study and

JACC Vol. 58, No. 19, 2011
November 1, 2011:1989–97

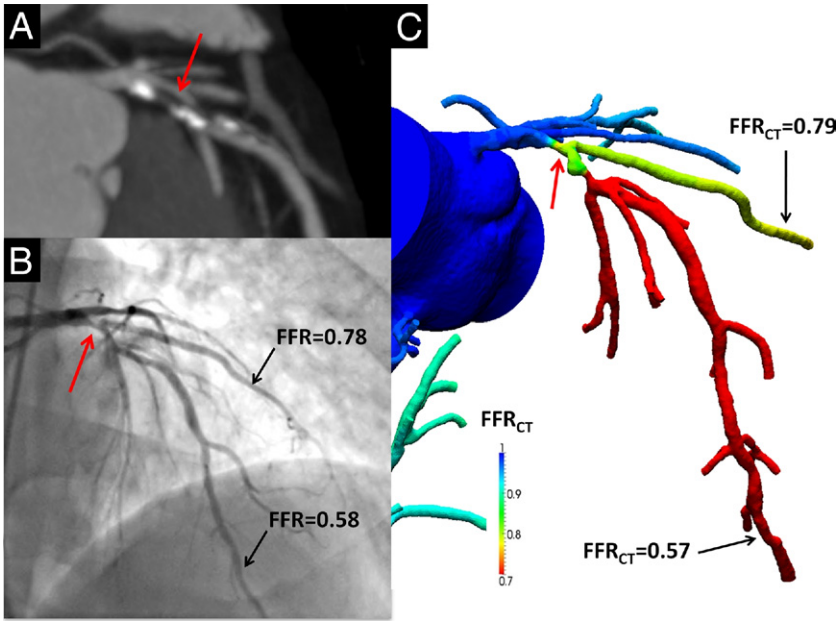

Figure 2 **Anatomically Obstructive Stenosis With a Lesion Causal of Ischemia**

(A) Multiplanar reformat of coronary computed tomography angiography demonstrating obstructive (≥50%) stenosis **(white arrow)** in the proximal portion of the left anterior descending (LAD) artery. **(B)** Invasive coronary angiography confirms the LAD stenosis **(red arrow)** with corresponding hemodynamically significant reductions in coronary pressure in the first diagonal branch (0.78) and distal LAD (0.58) by FFR. **(C)** Noninvasive computation of FFR from FFR_{CT} of the first diagonal branch (0.79) and distal LAD (0.57), demonstrating lesion-specific ischemia of the proximal LAD stenosis. Abbreviations as in Figure 1.

excluded them from the primary analysis to estimate the most conservative diagnostic performance of FFR_{CT}. Assignment of a value of 0.50 to FFR_{CT} would necessarily improve the performance of FFR_{CT} for vessels that would rarely be clinically interrogated by FFR_{CT} for ischemia. Post hoc analyses assigning these vessels a value of 0.50 did expectedly improve diagnostic performance with an accuracy, sensitivity, specificity, PPV, and NPV of 84.8%, 89.1%, 82.2%, 76.0%, and 92.2%, respectively.

Interestingly, 12 of 47 (25.5%) lesions judged to be of 50% to 69% stenosis severity by CCTA caused ischemia, as determined by an FFR ≤0.80. These results are in agreement with prior ICA-FFR studies wherein the magnitude of stenosis is often discordant with the presence of ischemia

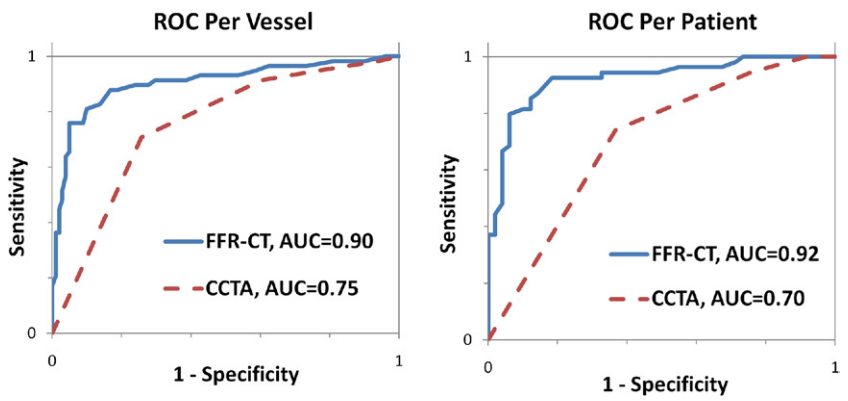

Figure 3 **ROC Demonstrating the AUC for FFR_{CT} and CCTA Stenosis for the Discrimination of Lesions That Cause Ischemia on a Per-Vessel and -Patient Level**

Areas under the receiver-operator characteristics curve (AUC) on a per-patient **(right)** and per-vessel **(left)** level for ischemia by fractional flow reserve ≤0.80 by coronary computed tomography angiography (CCTA) stenosis ≥50% or computation of fractional flow reserve from coronary computed tomographic angiography data (FFR_{CT}) ≤0.80. ROC = receiver-operator characteristic.

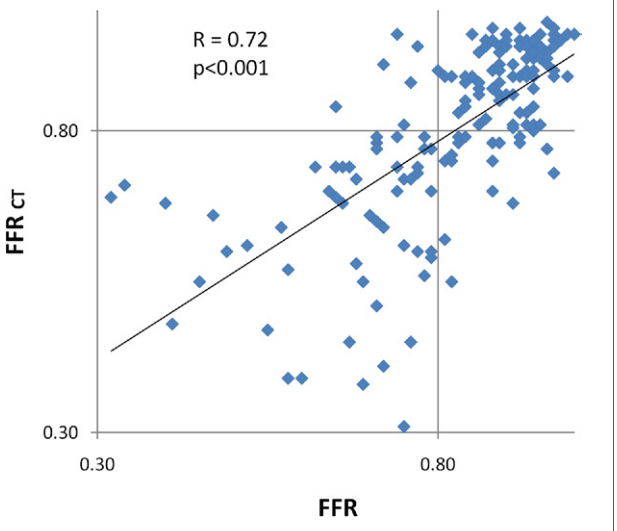

Figure 4 Correlation of FFR_{CT} to FFR

A good correlation (R = 0.72) is observed. Abbreviations as in Figure 1.

(31). These patients do not reach an angiographic threshold for revascularization but, nevertheless, experience ischemia (32). In these patients, the diagnostic performance of FFR_{CT} was maintained (accuracy 83.0%), and all 4 false negative lesions exhibited an invasive FFR value between 0.75 and 0.80, suggesting some degree of hemodynamic significance. The ability to noninvasively identify patients with ischemia but without high-grade stenoses might allow for more targeted treatments, and future studies examining this population should be considered.

We enrolled patients who did as well as did not have a prior history of CAD. Diagnostic performance of CCTA for anatomic CAD stenosis for patients with known CAD has been less robust than for patients with no prior history of CAD (8,9). As such, present Appropriate Use Criteria advocate the use of CCTA in the low-intermediate likelihood patient with suspected CAD, but the use of CCTA for patients with known CAD is generally considered uncertain or inappropriate (33). The addition of FFR_{CT} to CCTA measures of anatomic stenosis might enhance the diagnostic accuracy and expand the utility of CCTA in this population.

The findings of this study are of significant importance. Computation of FFR_{CT} from CCTAs might permit an "all-in-one" approach, whereby patient-specific stenosis can be assessed for lesion-specific ischemia. An FFR_{CT} might allow for enhanced detection of patients who might benefit from revascularization in a manner more specific than conventional stress perfusion imaging, which might manifest abnormalities due to epicardial stenosis or microvascular disease or both. Furthermore, radiation doses from cardiac imaging has recently been a topic of great discussion, and the computation of FFR_{CT} from typically acquired CCTA images negates the need for any additional ionizing radiation while providing combined physiological assessment of CAD (34). Finally, future evaluation of FFR_{CT} for prediction of hemodynamic improvement after revascularization or functional assessment of mild diffuse CAD might expand the clinical indications of this FFR_{CT} technique.

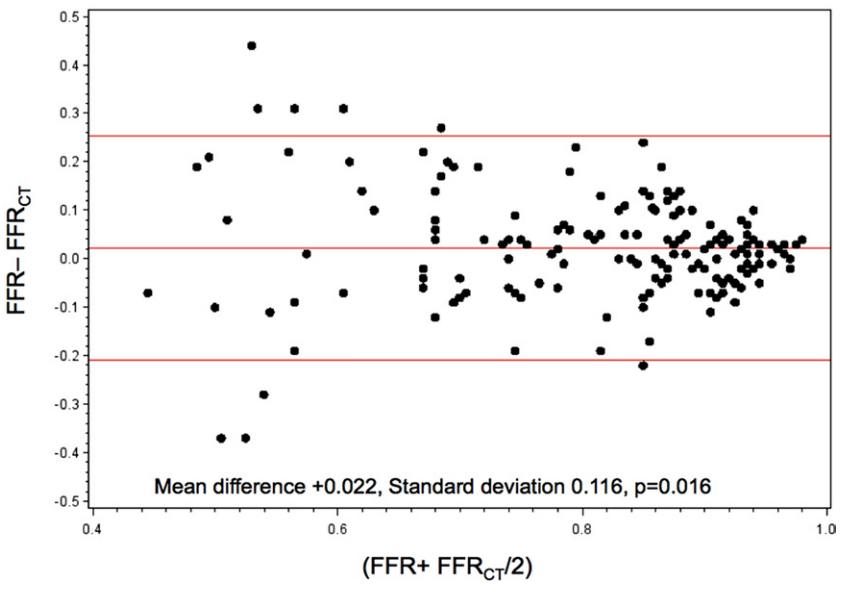

Figure 5 Bland-Altman Plot of FFR and FFR_{CT} on a Per-Vessel Basis

A slight systematic underestimation of computation of fractional flow reserve from FFR_{CT} as compared with FFR is observed. Abbreviations as in Figure 1.

This study is not without limitations. First, our study was adequately powered to determine the performance of FFR_{CT} versus CCTA stenosis at the per-vessel rather than the per-patient level. Establishment of per-patient performance of FFR_{CT} versus CCTA will require a greater number of patients, and we are performing a parallel, prospective study to address this hypothesis (35). Second, this study enrolled patients undergoing clinically indicated ICA and FFR, and thus the ability to assess the diagnostic performance of FFR_{CT} in all consecutive patients undergoing CCTA is not possible. However, ethical considerations precluded our performing ICA and FFR in patients for whom no significant CAD was present. Third, our study excluded patients with prior CABG, and thus the utility of FFR_{CT} in this population remains unknown. The FFR_{CT} should permit evaluation of CABG stenosis, by using the same principles applied to native coronary arteries, but future studies will be required to determine its diagnostic performance in this population.

Conclusions

In this prospective multicenter study, noninvasive FFR derived from typically acquired CCTA images offers a novel method that demonstrates high diagnostic performance for detection and exclusion of coronary artery lesions that cause ischemia.

Reprint requests and correspondence: Dr. James K. Min, Division of Cardiology, Department of Medicine, Cedars-Sinai Medical Center, 8700 Beverly Boulevard, South Taper Building 1258, Los Angeles, California 90048. E-mail: James.Min@cshs.org.

REFERENCES

1. DeBruyne B, Baudhuin T, Melin JA, et al. Coronary flow reserve calculated from pressure measurements in humans. Validation with positron emission tomography. Circulation 1994;89:1013–22.
2. Berger A, Botman KJ, MacCarthy PA, et al. Long-term clinical outcome after fractional flow reserve-guided percutaneous coronary intervention in patients with multivessel disease. J Am Coll Cardiol 2005;46:438–42.
3. Tonino PA, DeBruyne B, Pijls NH, et al. Fractional flow reserve versus angiography for guiding percutaneous coronary intervention. N Engl J Med 2009;360:213–24.
4. Pijls NH, van Son JA, Kirkeeide RL, DeBruyne B, Gould KL. Experimental basis of determining maximum coronary, myocardial, and collateral blood flow by pressure measurements for assessing functional stenosis severity before and after percutaneous transluminal coronary angioplasty. Circulation 1993;87:1354–67.
5. Fearon WF, Bornschein B, Tonino PA, et al. Economic evaluation of fractional flow reserve-guided percutaneous coronary intervention in patients with multivessel disease. Circulation 2010;122:2545–50.
6. Pijls NH, Fearon WF, Tonino PA, et al. Fractional flow reserve versus angiography for guiding percutaneous coronary intervention in patients with multivessel coronary artery disease: 2-year follow-up of the FAME (Fractional Flow Reserve Versus Angiography for Multivessel Evaluation) study. J Am Coll Cardiol 2010;56:177–84.
7. Min JK, Shaw LJ, Berman DS. The present state of coronary computed tomography angiography a process in evolution. J Am Coll Cardiol 2010;55:957–65.
8. Budoff MJ, Dowe D, Jollis JG, et al. Diagnostic performance of 64-multidetector row coronary computed tomographic angiography for evaluation of coronary artery stenosis in individuals without known coronary artery disease: results from the prospective multicenter ACCURACY (Assessment by Coronary Computed Tomographic Angiography of Individuals Undergoing Invasive Coronary Angiography) trial. J Am Coll Cardiol 2008;52:1724–32.
9. Miller JM, Rochitte CE, Dewey M, et al. Diagnostic performance of coronary angiography by 64-row CT. N Engl J Med 2008;359:2324–36.
10. Meijboom WB, Meijs MF, Schuijf JD, et al. Diagnostic accuracy of 64-slice computed tomography coronary angiography: a prospective, multicenter, multivendor study. J Am Coll Cardiol 2008;52:2135–44.
11. Meijboom WB, Van Mieghem CA, van Pelt N, et al. Comprehensive assessment of coronary artery stenoses: computed tomography coronary angiography versus conventional coronary angiography and correlation with fractional flow reserve in patients with stable angina. J Am Coll Cardiol 2008;52:636–43.
12. Lauer MS. CT angiography: first things first. Circ Cardiovasc Imaging 2009;2:1–3.
13. Redberg RF, Walsh J. Pay now, benefits may follow—the case of cardiac computed tomographic angiography. N Engl J Med 2008;359:2309–11.
14. Kim HJ, Vignon-Clementel IE, Coogan JS, Figueroa CA, Jansen KE, Taylor CA. Patient-specific modeling of blood flow and pressure in human coronary arteries. Ann Biomed Eng 2010;38:3195–209.
15. Kim HJ, Jansen KE, Taylor CA. Incorporating autoregulatory mechanisms of the cardiovascular system in three-dimensional finite element models of arterial blood flow. Ann Biomed Eng 2010;38:2314–30.
16. Kim HJ, Vignon-Clementel IE, Figueroa CA, et al. On coupling a lumped parameter heart model and a three-dimensional finite element aorta model. Ann Biomed Eng 2009;37:2153–69.
17. Abbara S, Arbab-Zadeh A, Callister TQ, et al. SCCT guidelines for performance of coronary computed tomographic angiography: a report of the Society of Cardiovascular Computed Tomography Guidelines Committee. J Cardiovasc Comput Tomogr 2009;3:190–204.
18. Raff GL, Abidov A, Achenbach S, et al. SCCT guidelines for the interpretation and reporting of coronary computed tomographic angiography. J Cardiovasc Comput Tomogr 2009;3:122–36.
19. Scanlon PJ, Faxon DP, Audet AM, et al. ACC/AHA guidelines for coronary angiography. A report of the American College of Cardiology/American Heart Association Task Force on practice guidelines (Committee on Coronary Angiography). J Am Coll Cardiol 1999;33:1756–824.
20. DeBruyne B, Pijls NH, Barbato E, et al. Intracoronary and intravenous adenosine 5'-triphosphate, adenosine, papaverine, and contrast medium to assess fractional flow reserve in humans. Circulation 2003;107:1877–83.
21. Vignon-Clementel IE, Figueroa CA, Jansen KE, Taylor CA. Outflow boundary conditions for 3D simulations of non-periodic blood flow and pressure fields in deformable arteries. Comput Methods Biomech Biomed Engin 2010;13:625–40.
22. Murray CD. The physiological principle of minimum work: I. The vascular system and the cost of blood volume. Proc Natl Acad Sci U S A 1926;12:207–14.
23. Hutchins GM, Miner MM, Boitnott JK. Vessel caliber and branch-angle of human coronary artery branch-points. Circ Res 1976;38:572–6.
24. Zhou Y, Kassab GS, Molloi S. In vivo validation of the design rules of the coronary arteries and their application in the assessment of diffuse disease. Phys Med Biol 2002;47:977–93.
25. Kamiya A, Togawa T. Adaptive regulation of wall shear stress to flow change in the canine carotid artery. Am J Physiol 1980;239:H14–21.
26. Zarins CK, Zatina MA, Giddens DP, Ku DN, Glagov S. Shear stress regulation of artery lumen diameter in experimental atherogenesis. J Vasc Surg 1987;5:413–20.
27. Wilson RF, Wyche K, Christensen BV, Zimmer S, Laxson DD. Effects of adenosine on human coronary arterial circulation. Circulation 1990;82:1595–606.
28. Chow BJ, Abraham A, Wells GA, et al. Diagnostic accuracy and impact of computed tomographic coronary angiography on utilization of invasive coronary angiography. Circ Cardiovasc Imaging 2009;2:16–23.
29. Patel MR, Peterson ED, Dai D, et al. Low diagnostic yield of elective coronary angiography. N Engl J Med 2010;362:886–95.

30. MacCarthy P, Berger A, Manoharan G, et al. Pressure-derived measurement of coronary flow reserve. J Am Coll Cardiol 2005;45: 216–20.
31. Tonino PA, Fearon WF, DeBruyne B, et al. Angiographic versus functional severity of coronary artery stenoses in the FAME study fractional flow reserve versus angiography in multivessel evaluation. J Am Coll Cardiol 2010;55:2816–21.
32. Bugiardini R, Bairey Merz CN. Angina with "normal" coronary arteries: a changing philosophy. JAMA 2005;293:477–84.
33. Taylor AJ, Cerqueira M, Hodgson JM, et al. ACCF/SCCT/ACR/AHA/ASE/ASNC/NASCI/SCAI/SCMR 2010 appropriate use criteria for cardiac computed tomography. A report of the American College of Cardiology Foundation Appropriate Use Criteria Task Force, the Society of Cardiovascular Computed Tomography, the American College of Radiology, the American Heart Association, the American Society of Echocardiography, the American Society of Nuclear Cardiology, the North American Society for Cardiovascular Imaging, the Society for Cardiovascular Angiography and Interventions, and the Society for Cardiovascular Magnetic Resonance. J Am Coll Cardiol 2010;56:1864–94.
34. Einstein AJ. Radiation risk from coronary artery disease imaging: how do different diagnostic tests compare? Heart 2008;94:1519–21.
35. Min JK, Berman DS, Budoff MJ, et al. Rationale and design of the DeFACTO (Determination of Fractional Flow Reserve by Anatomic Computed Tomographic Angiography) study. J Cardiovasc Comput Tomogr 2011;5:301–9.

Key Words: computational fluid dynamics ■ coronary CT angiography ■ fractional flow reserve.